REPORT DOCUMENTATION PAGE

Form Approved
OMB No. 0704-0188

1a REPORT SECURITY CLASSIFICATION: Unclassified	1b. RESTRICTIVE MARKINGS:
2a SECURITY CLASSIFICATION AUTHORITY	3. DISTRIBUTION/AVAILABILITY OF REPORT: Approved for public release; distribution unlimited
2b DECLASSIFICATION/DOWNGRADING SCHEDULE	
4 PERFORMING ORGANIZATION REPORT NUMBER(S): ASR-2	5. MONITORING ORGANIZATION REPORT NUMBER(S):
6a. NAME OF PERFORMING ORGANIZATION: The University of Texas at Austin; 6b. OFFICE SYMBOL (If applicable):	7a. NAME OF MONITORING ORGANIZATION: Office of Naval Research
6c. ADDRESS (City, State, and ZIP Code): Department of Mechanical Engineering, The University of Texas at Austin, Austin, TX 78712-1063	7b. ADDRESS (City, State, and ZIP Code): Physics Division - Code 1112, Arlington, VA 22217-5000
8a. NAME OF FUNDING/SPONSORING ORGANIZATION; 8b. OFFICE SYMBOL (If applicable):	9. PROCUREMENT INSTRUMENT IDENTIFICATION NUMBER: N00014-85-K-0708
8c. ADDRESS (City, State, and ZIP Code):	10. SOURCE OF FUNDING NUMBERS: PROGRAM ELEMENT NO. 61153N 11; PROJECT NO.; TASK NO. 4126943; WORK UNIT ACCESSION NO.

11 TITLE (Include Security Classification)
Problems in Nonlinear Acoustics: Parametric Receiving Arrays, Focused Finite Amplitude Sound, and Noncollinear Tone-Noise Interactions

12 PERSONAL AUTHOR(S)
Mark F. Hamilton

13a TYPE OF REPORT	13b. TIME COVERED	14. DATE OF REPORT (Year, Month, Day)	15. PAGE COUNT
Annual Summary	FROM 860501 TO 870701	870701	32

16. SUPPLEMENTARY NOTATION

17. COSATI CODES			18. SUBJECT TERMS (Continue on reverse if necessary and identify by block number)
FIELD	GROUP	SUB-GROUP	nonlinear acoustics; parametric array; scattering of sound by sound; focused sound; waveguide; noise

19 ABSTRACT (Continue on reverse if necessary and identify by block number)

Three projects are discussed in this annual summary report. (1) Parametric Receiving Arrays. This project is a theoretical investigation into the use of a parametric receiving array for directive measurements of noise radiated by ships in reverberant environments. The analysis is based on a Gaussian beam model that takes nearfield diffraction into account. The scattering of sound by sound is also investigated. (2) Focused Finite Amplitude Sound. A numerical solution is used to investigate the combined effects of nonlinearity, diffraction, and absorption on sound that propagates through a focal region. The analysis yields time waveforms, axial propagation curves, spectral power distributions, and beam patterns. (3) Noncollinear Tone-Noise Interactions. The noncollinear interaction of a pure tone and a band of noise that propagate in different modes of a rectangular duct is investigated both experimentally and theoretically.

20. DISTRIBUTION/AVAILABILITY OF ABSTRACT: ☒ UNCLASSIFIED/UNLIMITED ☐ SAME AS RPT. ☐ DTIC USERS	21. ABSTRACT SECURITY CLASSIFICATION: Unclassified
22a NAME OF RESPONSIBLE INDIVIDUAL: L. E. Hargrove	22b. TELEPHONE (Include Area Code): (202)696-4221; 22c. OFFICE SYMBOL: ONR Code 1112

DD Form 1473, JUN 86 *Previous editions are obsolete.*

TABLE OF CONTENTS

PROBLEMS IN NONLINEAR ACOUSTICS:

PARAMETRIC RECEIVING ARRAYS, FOCUSED FINITE AMPLITUDE SOUND, and NONCOLLINEAR TONE-NOISE INTERACTIONS

Second Annual Summary Report
ONR Contract N00014-85-K-0708
1 July 1987

Mark F. Hamilton

INTRODUCTION

This annual summary report describes research performed from 1 May 1986 until 1 July 1987 under ONR Contract N00014-85-K-0708, which began 1 September 1985. The following projects are discussed:

1. Parametric Receiving Arrays
2. Focused Finite Amplitude Sound
3. Noncollinear Tone-Noise Interactions

All three projects involve basic research on nonlinear acoustics. The first project is a theoretical investigation of the use of a parametric receiving array for measuring ship noise. We are primarily concerned with the effect of reflecting surfaces on nonlinear interactions in the nearfield of diffracting sound beams. The second project, which is essentially completed, is a numerical investigation of the combined effects of nonlinearity and diffraction on sound that propagates through a focal region. The third project is an experimental investigation of the interaction between a pure tone in the (1,0) mode of a rectangular duct and a band of noise in the (0,0) mode. This last project received direct support from ONR only prior to 1 June 1986.

The following individuals are involved with the research effort:

Senior Personnel

M. F. Hamilton, principal investigator

Graduate Students

C. Darvennes, Ph.D. student in Mechanical Engineering

T. S. Hart, M.S. student in Electrical and Computer Engineering

S. J. Lind, M.S. student in Architectural Engineering

I. PARAMETRIC RECEIVING ARRAYS

The purpose of this research is to investigate the use of a parametric receiving array for directive measurements of noise radiated by ships in reverberant environments. The investigation is theoretical and has been performed by Darvennes since 1 September 1985. Our primary objective is to develop a mathematical model that takes into account multipath components from reflecting surfaces. Both theoretical and experimental investigations of related problems are currently underway at Applied Research Laboratories of the University of Texas at Austin (ARL:UT) and the Department of Mathematics at the University of Bergen, Bergen, Norway. We are in close contact with both groups, and their contributions are discussed briefly below.

A. Background

The proposed application of a parametric receiving array to the problem of measuring noise radiated by large ships underway in reverberant environments is outlined in detail in the First Annual Summary Report [1]. The problem may be summarized as follows. Measurement of ship noise is complicated by multipath arrivals from both the ocean floor and the surface of the water. The reflections make it difficult to calculate either the source level or directivity pattern. Moreover, when the ship is in motion, each multipath component may experience a different Doppler shift, with the result that the frequency distribution of energy in the received signal differs from that transmitted by the ship. A highly directional hydrophone array is therefore needed if elimination of the multipath components is desired. Because of its relative insensitivity to differential Doppler shift and its potentially high directivity, an end-fire array presents itself as a viable means of discriminating against the undesirable multipath components. However, at the low frequencies characteristic of ship noise, an array hundreds of meters in length may be necessary.

A parametric receiving array has been suggested [2] as a possible solution to the problem (see Fig. 1). The receiver consists of only two components: a directive, high power pump transducer and a hydrophone. A high intensity beam is transmitted by the pump through the noise field. The beam interacts nonlinearly with the noise, and modulation components (sum and difference frequency sidebands) are received by the hydrophone. Information about the directional properties of the noise field is carried by the nonlinearly generated sidebands. The column of water between the source and hydrophone, which in theory may be arbitrarily

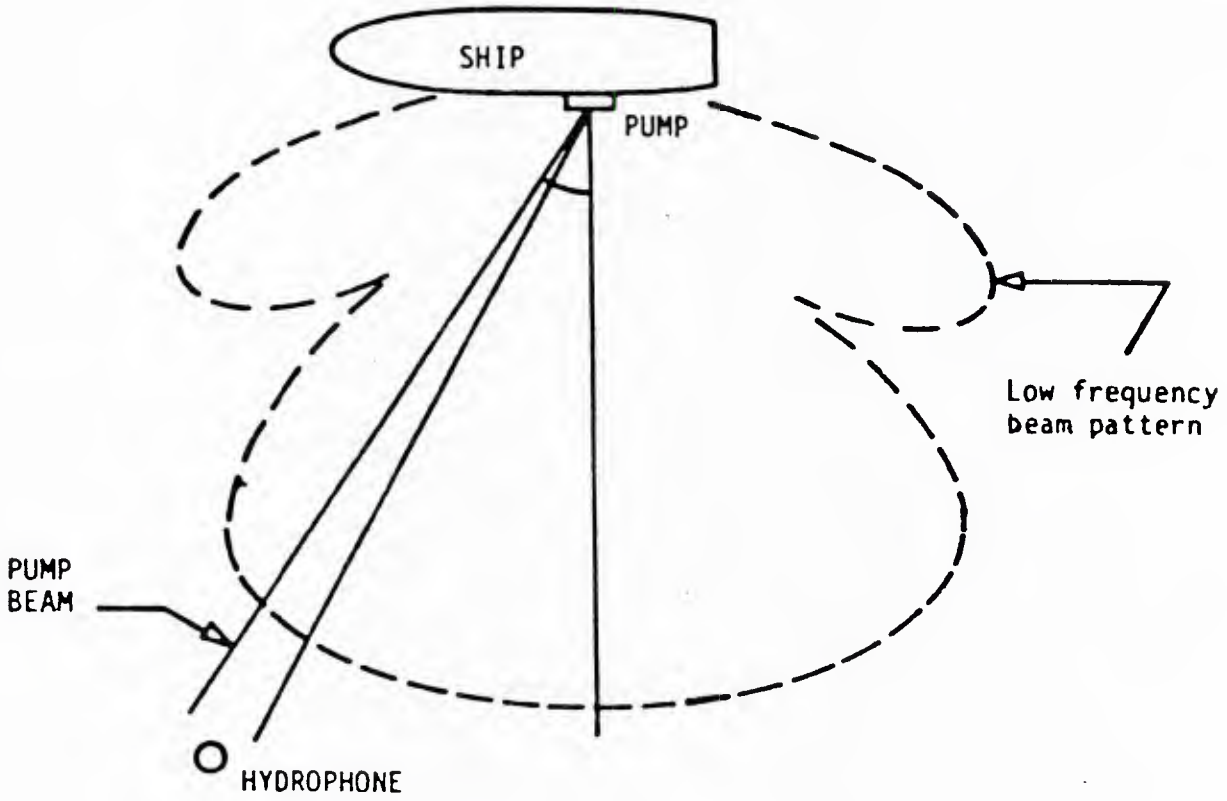

Figure 1

Parametric receiving array used to measure ship noise

long, thus synthesizes elements of a continuous, end-fire line array. Steering the array would be accomplished by mounting the pump on the ship itself, with the hydrophone placed at a fixed location some distance away. Navigation data provided by the ship may be employed to continuously direct the pump toward the hydrophone.

Until recently, theoretical models of parametric receivers did not account for diffraction of the noise field. Although one model [3] accounted for diffraction of the pump beam, the noise field was assumed to consist only of plane waves. However, the noise field radiated by a large ship may have a nearfield hundreds of meters long. Since the scheme for measuring the ship noise with a parametric receiver involves mounting the pump directly on the ship, nearfield diffraction effects in the noise field cannot be ignored. A Gaussian beam model of parametric reception that accounts for both diffraction of the pump wave and the noise field was developed by Hamilton, Naze Tjøtta, and Tjøtta [4]. It was assumed that both the pump beam and noise field are pure tones, and that both are radiated from sources with Gaussian amplitude distributions. The solution is particularly attractive because it is expressed in closed form in terms of exponential integral functions, and it is therefore very easy to evaluate on a computer.

Considerable progress has been made over the past year in the Department of Mathematics at the University of Bergen. In a paper by Foote, Naze Tjøtta, and Tjøtta [5], the restriction of Gaussian beams is removed. Specifically, pumps and sources having circular geometries with uniform amplitude distributions are considered. The penalty is that numerical solution of a triple integral is required. One conclusion of the analysis is that results obtained with Gaussian pumps and uniform pumps are virtually indistinguishable. The main focus of the paper, however, is the effect of misalignment between the pump and hydrophone, a practical problem when the distance between the pump and hydrophone is large.

At ARL:UT, Sample [6,7] has investigated arbitrary source distributions by using a superposition of Gaussian sources in order to take advantage of the closed form solution in Ref. 4. To test his method, Sample used Gaussian beams to model radiation from a uniform circular source and investigated the resulting nonlinear interaction with sound from a Gaussian pump. The results compare favorably with those of Foote *et al.* [5], thus verifying the approach. Two significant advantages result from the method of Gaussian superposition. First, complicated source distributions associated with large structures, such as hulls of ships,

can be modeled. Second, the calculations require relatively little computation time. These advantages are useful for evaluating engineering and design considerations associated with deployment of the parametric receiver.

Finally, ARL:UT is now beginning experimental work on nearfield parametric reception. The experiment will involve the use of a parametric receiving array to measure sound radiated from a large uniform circular source. Results from the experiment should provide important comparisons with the theoretical models.

The following results were obtained during the past year under the current ONR contract. Some of the results were presented orally by Darvennes and Hamilton [8] at a meeting of the Acoustical Society of America. Our main objective is to determine the extent to which a parametric receiver discriminates against multipath components in diffracting sound fields. This aspect of the problem has not been addressed in any of the previous work on nearfield parametric reception [4–7]. However, knowledge of how a parametric receiver performs in a reverberant environment is crucial for interpreting results when measuring ship noise. Related work on parametric interactions near reflecting surfaces has been performed by Novikov, Tarasov, and Timoshenko [9], although transmitting instead of receiving parametric arrays were investigated. The problem of parametric reception near reflecting surfaces has been considered by Donskoi and coworkers [10–12], but the results do not account for nearfield diffraction.

B. Results

A quasilinear analysis was used to investigate the nonlinear interaction of two Gaussian beams whose sources may be displaced and tilted with respect to each other. The spatial component of the source function for the ith primary wave ($i = 1, 2$) is assumed to be

$$p_i(\mathbf{r}, 0) = p_{0i} \exp\left(-\frac{|\mathbf{r} - \mathbf{b}_i|^2}{\epsilon_i^2} - jk_i x \sin\theta_i\right) \tag{1}$$

where the time factor $\exp(j\omega_i t)$ is suppressed, and p_{0i} is the on-source pressure amplitude, $\mathbf{r}$ a position vector in the x–y plane, ϵ_i the radius of the source, $\mathbf{b}_i$ the displacement of the source from the z axis, $k_i = \omega_i/c_0$ the wavenumber, ω_i the angular frequency, and θ_i the angle of rotation. Thus for $\mathbf{b}_i = \mathbf{0}$ and $\theta_i = 0$, the ith beam is directed along the z axis. Positive values of θ_i indicate clockwise rotation with respect to the z axis. The pump is designated by $i = 1$ and the noise source by $i = 2$.

When effects of thermoviscous absorption can be ignored, the solution for the difference frequency field ($\omega_- = \omega_1 - \omega_2$) in the paraxial region may be written in the form

$$p_-(\mathbf{r}, z) = f(\mathbf{r}, z)(E_1[g(\mathbf{r}, z)] - E_1[h(\mathbf{r}, z)]) , \tag{2}$$

where E_1 is the exponential integral function, and f, g, and h are simple algebraic functions of the system parameters. Equation (2) is an important generalization of the result derived in Ref. 4, where a closed form result is obtained only along the acoustic axis of one of the interacting beams.

The generation of difference (or sum) frequency sound by two beams that interact at a nonzero angle is referred to as the *scattering of sound by sound* (see, *e.g.*, Refs. 13 and 14 for a review). Whether the difference frequency sound can be radiated *outside* the noncollinear interaction region formed by the intersecting primary beams has fueled controversy in the nonlinear acoustics community ever since the problem was first posed in 1956 [15]. It is also worth noting that over the past three decades, ONR has supported some of the most prominent research on the scattering of sound by sound [16–19].

Equation (2) is apparently the first closed form solution of the scattering of sound by sound that takes nearfield diffraction into account. Here we consider a specific example. Shown in Fig. 2 is the geometry and notation for two beams that interact at angle $(\theta_2 - \theta_1)$. We have analyzed the scattering of sound by sound for the following parameter values: $\theta_2 = -\theta_1$, $\omega_1/\omega_2 = 3$, $k_2\epsilon_2 = 30$, $\epsilon_1 = \epsilon_2$, $\mathbf{b}_1 = 1.5\epsilon_1\mathbf{e}_x$, and $\mathbf{b}_2 = -1.5\epsilon_2\mathbf{e}_x$. Under these conditions, the effective edges of the sources are separated by one radius. Shown in Fig. 3 are beam patterns for the difference frequency field when the interaction angles are $10°$ ($\theta_2 = -\theta_1 = 5°$) and $20°$ ($\theta_2 = -\theta_1 = 10°$). The dimensionless range $Z = 2z/k_2\epsilon_2^2$ is in terms of the collimation length of the lower frequency primary beam.

The most interesting characteristic of the difference frequency beam patterns is the appearance of two sidelobes, and it turns out that the location of each sidelobe is easily predicted. As the observation range Z increases, the right-hand sidelobe in each beam pattern is described asymptotically by the product directivity function $D_1(\theta)D_2(\theta)$, where $D_i(\theta)$ is the directivity function of the ith primary wave. The function $D_1(\theta)D_2(\theta)$ is maximized at $\theta = -4°$ when the beams interact at $10°$, and at $\theta = -8°$ when the interaction angle is $20°$. Since the right-hand sidelobe is always located between θ_1 and θ_2, it can be argued that sound in this sidelobe is not outside the interaction region.

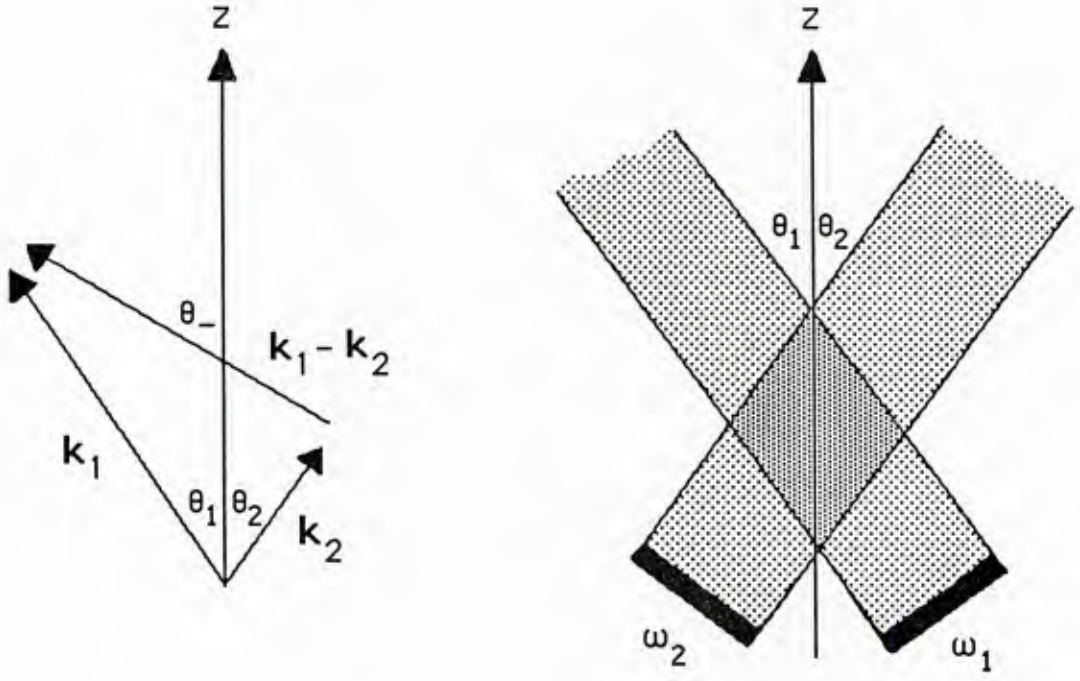

Figure 2

Scattering of sound by sound

Beam interaction angle = 10° ($\theta_2 = -\theta_1 = 5°$)

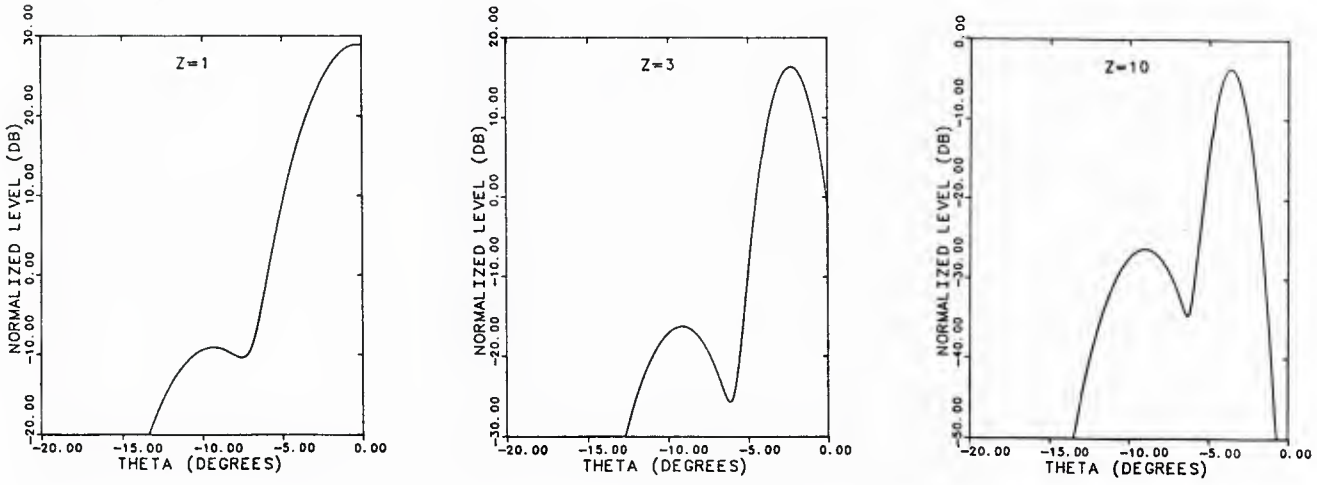

Beam interaction angle = 20° ($\theta_2 = -\theta_1 = 10°$)

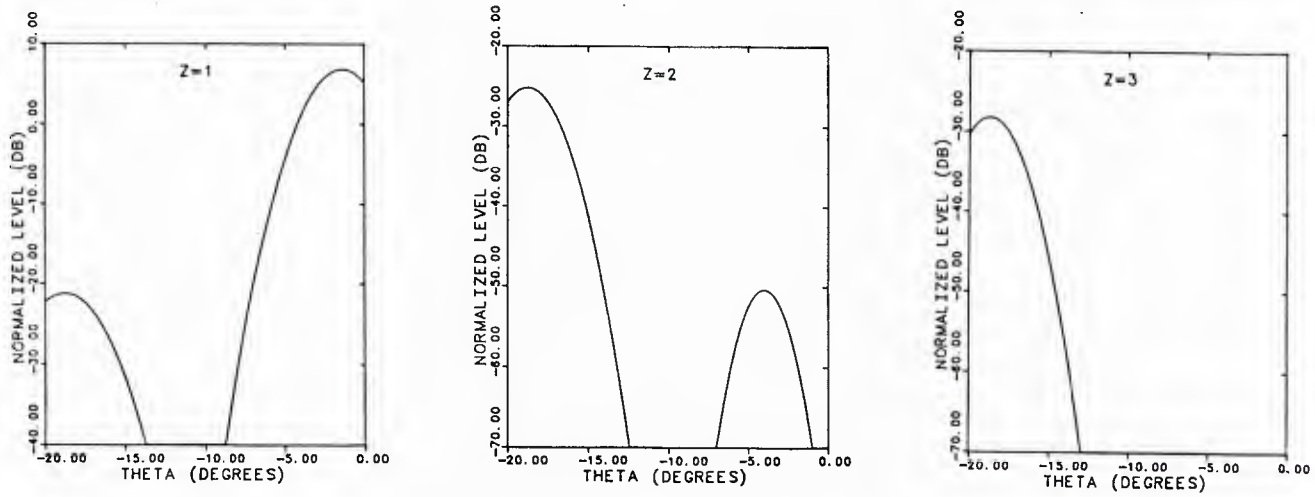

Figure 3

Beam patterns for scattered difference frequency sound

In contrast, the left-hand sidelobe is centered at $\theta = \theta_-$, which is seen in Fig. 2 to be the direction of the vector $\mathbf{k}_1 - \mathbf{k}_2$. The angle θ_- is always outside the region defined by the directions of the two primary beams. Specifically, we obtain $\theta_- = -10°$ when $\theta_1 = -5°$ and $\theta_- = -19°$ when $\theta_1 = -10°$. For small interaction angles, the contribution from the product directivity dominates the beam pattern. At an interaction angle of 20°, however, the sidelobe at θ_- eventually dominates the field. Moreover, the level of the sidelobe at θ_- can be substantial. For example, if two Gaussian primary beams interact in air at 20° with on-source levels of approximately 145 dB (*re*: 20 μPa), the sound pressure level of the sidelobe at $Z \approx 2$ and $\theta \approx -19°$ should be approximately 73 dB.

More germane to the research on parametric reception is the application of Eq. (2) to the problem of noncollinear interaction of two sound fields in the presence of a reflecting surface. If the pump wave is sufficiently well collimated that its reflection from the surface of the water may be ignored, then the only reflections that need to be considered are those due to the noise field and the difference frequency field. In this limiting case, the difference frequency field due to the interaction of the pump wave and the noise field may be constructed using the method of images. The resulting solution is given by the summation of four equations that have the same general form as Eq. (2). Figure 4 depicts the four basic interactions which are taken into account. The pump wave interacts with both the direct (a, c) and reflected (b, d) source wave, and the resulting difference frequency sound takes both a direct (a, b) and reflected (c, d) path on its way to the hydrophone. This solution is valid when the distance from the pump to the hydrophone is not too large, such that neither absorption nor reflection of the pump wave need be taken into account.

As an example we use the following parameters: $k_2\epsilon_2 = 30$ (dimensionless source radius), $k_1/k_2 = 1000$ (for example, 50 Hz for the source frequency and 50 kHz for the pump frequency), and $\epsilon_2/\epsilon_1 = 50$ (therefore $k_1\epsilon_1 = 600$ is the dimensionless pump radius). Practical design considerations for constructing a parametric receiver with similar parameters are discussed by McDonough [20]. Results are shown in Fig. 5 for a source at depths $2\epsilon_2$ and $5\epsilon_2$ below the surface of the water. Increasing θ corresponds to moving the observation point away from the surface. The solid curves in the top two figures are farfield beam patterns that would be measured linearly with a point receiver, and the dashed curves are the corresponding free field directivities. The oscillations in the beam patterns are due to reflected multipath components.

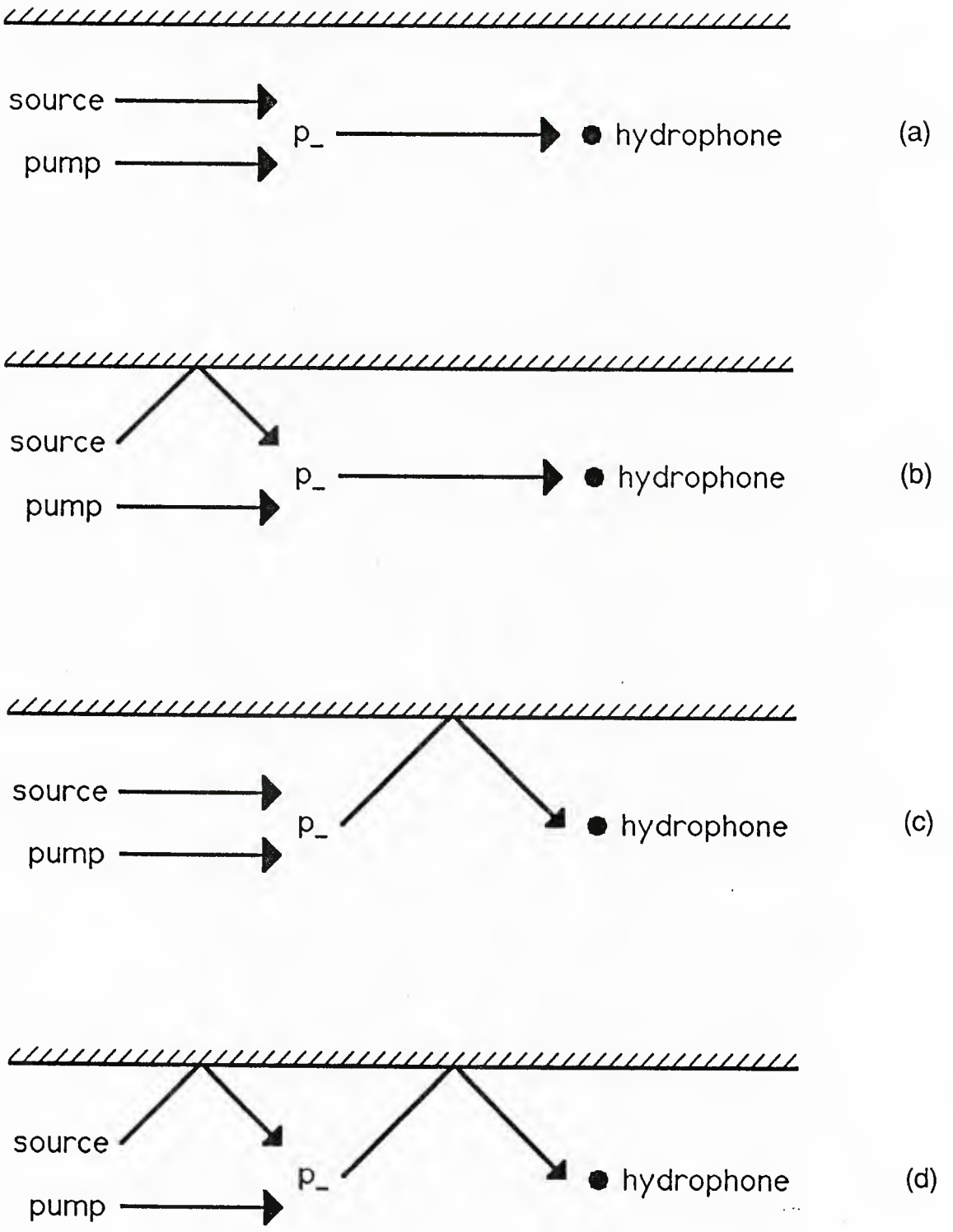

Figure 4

Pump/source wave interactions near a reflecting boundary

source depth = $2\varepsilon_2$

source depth = $5\varepsilon_2$

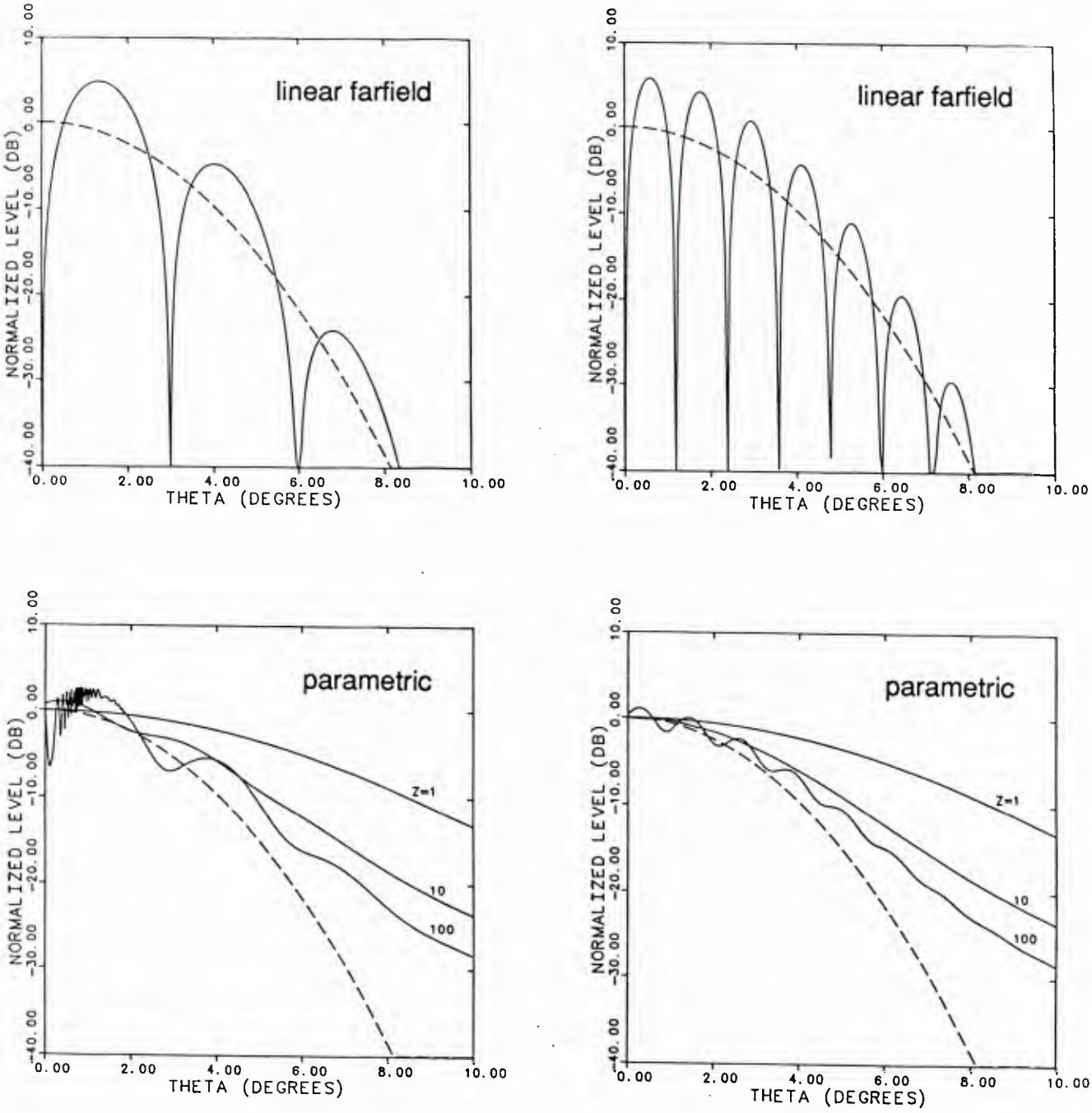

Figure 5

Beam patterns near a pressure release surface

The bottom two figures show beam patterns measured by a parametric receiver with the pump mounted in the center of the source, and with the hydrophone at various dimensionless ranges $Z = 2z/k_2\epsilon_2^2$ (*i.e.*, in terms of the Rayleigh distance of the source). Close to the source ($Z = 1$) there are no oscillations in the measured beam patterns, but the source beamwidth is significantly overestimated (see Ref. 4). At $Z = 10$ the predicted beamwidth is somewhat better, and there is still reasonably strong discrimination against multipath. However, multipath is seen to significantly affect the parametrically measured beam pattern when $Z = 100$, more so when the source is closer to the surface. The large oscillations that resemble those in the linear farfield beam patterns result from interaction (b) in Fig. 4. The rapid oscillations at $\theta < 2°$ for a source at depth $2\epsilon_2$ are due to interaction (c).

A trade-off thus exists in terms of the optimum range for measuring beam patterns with a parametric receiver in multipath environments. When the hydrophone is too close to the source, the beamwidth may be significantly overestimated. However, multipath increasingly contaminates parametric reception as the hydrophone is moved farther away. The optimum range for the hydrophone depends on a combination of factors. As we have seen, one factor is the distance of the source from the reflecting surface. Other factors involve the frequency and thermoviscous absorption of the pump wave.

The more general solution, *i.e.*, when absorption and reflection of the pump wave are taken into account, is based on an integral expression of the form

$$p_-(\mathbf{r}, z) = \int_0^z G(\mathbf{r}, z; z')\, dz' \,, \tag{3}$$

where G is a function that in turn depends on the error function. Now there are eight interactions which must be considered. In addition to the four shown in Fig. 4, an additional four involve reflection of the pump wave. The integral in Eq. (3) is difficult to evaluate numerically, and the problem is currently under investigation.

II. FOCUSED FINITE AMPLITUDE SOUND

This project consists of a numerical investigation begun by Hart on 1 September 1985. The task involves the modification of an existing computer program for application to finite amplitude sound that propagates through a focal region. The project is near completion, and a comprehensive account of the investigation is currently being written up as a masters thesis. Hart is scheduled to receive his M.S. degree in Electrical and Computer Engineering in August 1987.

A. Background

The problem we have analyzed involves the nonlinear distortion, diffraction, and absorption of sound as it propagates through a focal region. Only recently have these combined effects been taken into account simultaneously in investigations of unfocused sound fields. Previous theoretical research on focused finite amplitude sound has been reviewed in the First Annual Summary Report [1]. Here we describe only briefly where our results fit in with the current state of the art.

A numerical solution, similar to ours, has already been used by Bakhvalov *et al.* [21] to investigate nonlinear effects in focused sound fields (see also Chapter 4 of Ref. 22). Like our investigation, theirs is based on the Khokhlov-Zabolotskaya-Kuznetsov (KZK) equation [23,24]. Their analysis, however, does not take into account the abrupt edges that characterize circular piston transducers. Therefore the strong diffraction effects that appear in sound fields radiated by most circular ultrasonic transducers are not considered. The majority of sources analyzed by Bakhvalov *et al.* possess Gaussian amplitude distributions of the form $\exp(-r^2/a^2)$, where r is a radial coordinate and a is an effective source radius. As is well known, sound fields radiated by Gaussian sources exhibit neither an oscillatory nearfield structure nor a farfield sidelobe structure. The strongest diffraction effects considered by Bakhvalov *et al.* result from the fourth-order polynomial source distribution defined by $[1-(r/a)^2]$ for $r \leq a$ and zero for $r > a$. As shown in the First Annual Summary Report [1], the sound field that results from a fourth-order source function approximates only roughly the field from a circular piston. Finally, their investigation considers only focusing gains of order 5, whereas most interesting applications of focused sound involve focusing gains that are an order of magnitude larger.

In contrast, a theoretical study by Lucas and Muir [25,26], also based on the KZK equation, is limited to weakly nonlinear systems. However, the practical case of a focused circular source with gain of 40 is investigated. The authors obtain a quasilinear solution for the fundamental and second harmonic components that is in good agreement with experiment. The demonstrated ability of the KZK equation to accurately model focused sound fields from realistic sources (*i.e.*, having abrupt edges and high gains) lends credibility to our own investigation.

Thus the work of Bakhvalov *et al.* accounts for strong nonlinearity but weak diffraction and low focusing gains, and that of Lucas and Muir accounts for strong diffraction and high focusing gains but weak nonlinearity. The research described below bridges the gap by taking into account strongly nonlinear sound fields with high focusing gains and strong diffraction effects.

The following results have been presented orally by Hart and Hamilton [27] at a meeting of the Acoustical Society of America. The text is excerpted from a paper by Hart and Hamilton [28] that will appear in proceedings of the 11th International Symposium on Nonlinear Acoustics.

B. Results

In an earlier investigation, a transformation [29] of the KZK equation [23,24] was introduced that facilitates the numerical calculation of nonlinear effects in the farfield of directive sound beams. The transformation introduces a coordinate system that follows the eventual spherical divergence of collimated sound waves. Here we introduce a similar transformation which is suitable for describing the convergent geometry of focused sound fields.

Our analysis begins with the KZK equation written in the form

$$\left(\frac{\partial^2}{\partial\tau\partial\sigma} - \frac{d}{4z_0}\nabla_\perp^2 - \alpha d\frac{\partial^3}{\partial\tau^3}\right) P = \frac{d}{2l_p}\frac{\partial^2 P^2}{\partial\tau^2}, \tag{4}$$

where $\sigma = z/d$ is a dimensionless range in terms of the axial coordinate z and the focal length d, $\tau = \omega(t - z/c_0)$ is dimensionless retarded time where $\omega/2\pi$ is the source frequency and c_0 the sound speed, $P = p/p_0$ is a dimensionless pressure in terms of the acoustic pressure p and its on-source value p_0, $z_0 = \omega a^2/2c_0$ is the Rayleigh distance, a the source radius, α the absorption coefficient at angular frequency ω, and $l_p = \rho_0 c_0^3/\beta\omega p_0$ the plane wave shock

formation distance, where ρ_0 is the ambient density and β the coefficient of nonlinearity. The two-dimensional Laplace operator $\nabla_\perp^2$ is written in terms of the dimensionless vector $\mathbf{u} = \mathbf{r}/a$, where $\mathbf{r} = (x, y)$ is the transverse coordinate vector. The focal plane is defined to be at $\sigma = 0$, with the source located at $\sigma = -1$ and radiating in the $+\sigma$ direction (see Fig. 6).

Three dimensionless coefficients appear explicitly in Eq. (4), all of which involve the focal length d. The ratio $G \equiv z_0/d$ may be identified as the linear focusing gain. With the right hand side of Eq. (4) set to zero and with no absorption ($\alpha = 0$), the solution for radiation from a circular source yields an amplitude for P equal to G at the focus [25]. The quantity αd indicates the role of absorption within one focal length, and d/l_p is a dimensionless source amplitude.

To construct a coordinate system that converges at the focus, we introduce the transformation

$$P'(\sigma, \mathbf{u}', \tau') = (\sigma \pm \delta) P(\sigma, \mathbf{u}, \tau)\,, \qquad \mathbf{u}' = \frac{\mathbf{u}}{\sigma \pm \delta}\,, \qquad \tau' = \tau - \frac{u^2}{\sigma \pm \delta}\,, \tag{5}$$

where δ is a small positive quantity, and $u = |\mathbf{u}|$. The parameter δ governs the rate at which the primed geometry converges. With $\delta \ll 1$, length scales in the focal plane are δ times smaller than at the source. Note that the primed coordinates are singular in the focal plane when $\delta = 0$. The minus signs in Eqs. (5) are used in the prefocal region ($\sigma < 0$) and the plus signs beyond the focus ($\sigma > 0$). Substitution of Eqs. (5) in Eq. (4) yields

$$\left((\sigma \pm \delta)^2 \frac{\partial^2}{\partial \tau' \partial \sigma} - \frac{d}{4 z_0} \nabla_\perp'^2 - \alpha d (\sigma \pm \delta)^2 \frac{\partial^3}{\partial \tau'^3} \right) P' = \frac{d}{2 l_p} (\sigma \pm \delta) \frac{\partial^2 P'^2}{\partial \tau'^2}\,, \tag{6}$$

where $\nabla_\perp'^2$ is the two-dimensional Laplace operator with respect to $\mathbf{u}'$. With the quantity P' expanded in the series

$$P' = \sum_{n=-\infty}^{\infty} p'_n(\sigma, \mathbf{u}') e^{jn\tau'}\,, \tag{7}$$

Eq. (6) can be rewritten as the coupled set of equations

$$\frac{\partial p'_n}{\partial \sigma} = -n^2 \alpha d\, p'_n - \frac{jd}{4 n z_0 (\sigma \pm \delta)^2} \nabla_\perp'^2 p'_n + \frac{jnd}{2 l_p (\sigma \pm \delta)} \sum_{m=-\infty}^{\infty} p'_m p'_{n-m}\,. \tag{8}$$

The coupled parabolic equations in p'_n are solved via the implicit backward finite difference method described in Ref. 30. For an axisymmetric source having gain G and oscillating sinusoidally with amplitude distribution $f(u)$, the boundary condition at $\sigma = -1$ is, within

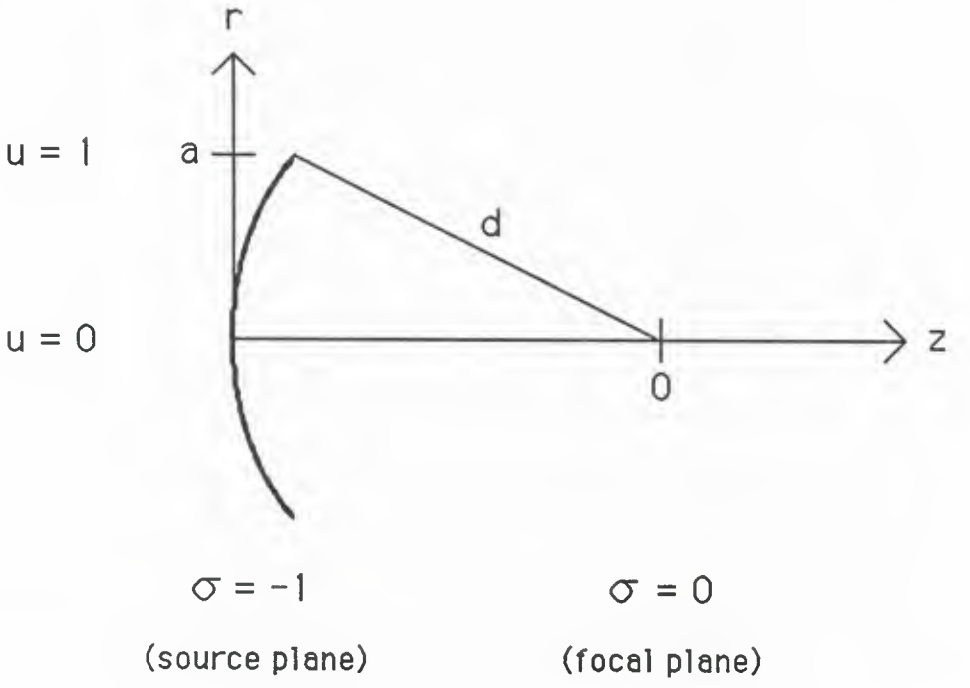

Figure 6

Geometry of focused source

the parabolic approximation, $P = f(u)\sin(\tau + Gu^2)$. In the primed system the boundary conditions become, where use is made of Eqs. (5) and (7), $p'_1 = (j\gamma/2)f(\gamma u')\exp j(\gamma^2 G - \gamma)u'^2$ (where $\gamma = 1 + \delta$), $p'_{-1} = p'^*_1$ (where the asterisk indicates complex conjugate), and $p'_n = 0$ for all $n \neq \pm 1$. With the minus signs selected in Eqs. (5) and (8), the finite difference algorithm steps forward from the source toward the focus. At the focus, the minus signs are changed to plus signs, the primed systems defined in Eqs. (5) are matched, and the algorithm resumes.

We now present results for focused sound from circular sources with amplitude distributions described by $f(u) = 1$ for $u < 1$ and $f(u) = 0$ for $u > 1$.

Shown in Fig. 7 are time waveforms calculated along the axis of a focusing system where $G = 72.5$, $\alpha d = 1.11$, and $d/l_p = 1.06$. The parameters are chosen to correspond with those of an investigation performed by Rugar [31], who used an acoustic microscope which transmits focused sound through liquid nitrogen at frequencies around 2 GHz. The dimensionless peak amplitude of the sinusoidal source waveform shown in Fig. 7(a) is unity. Note that the amplitude scale in (a) is magnified 10 times with respect to the scales in ($b - f$). After the wave enters the focal region (b), finite amplitude distortion increases dramatically (c, d). At the focus (d), the effect of using only 25 harmonics in the calculations is manifested as small ripples in the waveform. It is interesting to compare the peak amplitude of the wave at the focus with the result predicted by linear theory. The linear focusing gain of 72.5, multiplied by the attenuation factor $e^{-1.11}$, yields a dimensionless peak amplitude of 24 at the focus. Because of nonlinearity and diffraction, the compression peak in (d) is almost twice that amplitude, while the expansion trough is roughly half. Diffraction is responsible for the asymmetric shape of the wave. Comparison of (b) and (f) shows an approximately 180° phase shift of the peak as the wave propagates through the focus.

Shown in Fig. 8, as functions of $\sigma = z/d$, are the axial amplitudes for the fundamental through fourth harmonic components of the waveform in Fig. 7. As in subsequent figures, the solid line is for the fundamental component ($n = 1$), the long dashes for the second harmonic ($n = 2$), the short dashes for the third harmonic ($n = 3$), and the dotted line for the fourth harmonic ($n = 4$). Careful examination reveals that all components attain their peak amplitudes just before the focal plane. However, the maximum amplitude of the time waveform is attained slightly beyond the focus (not shown in Fig. 7).

Another point of view, one which supplements Fig. 8, is achieved by calculating the power

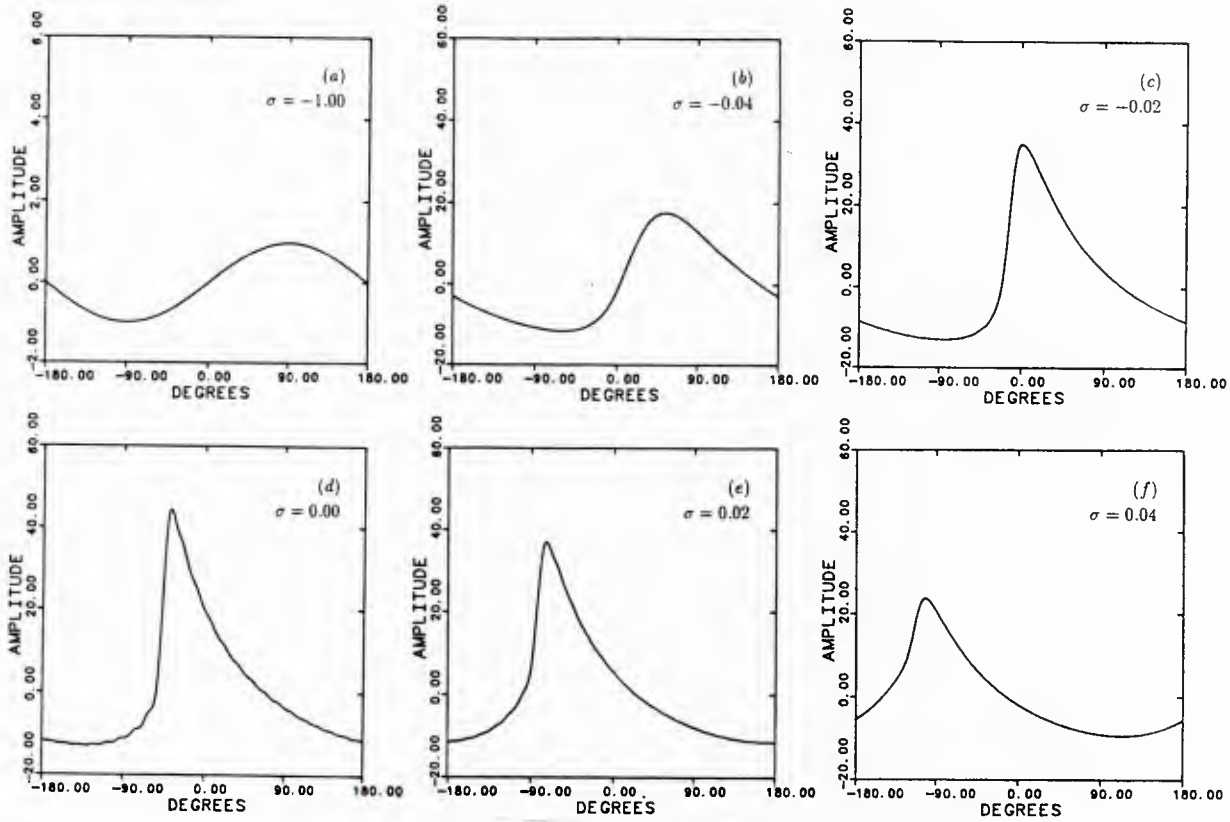

Figure 7

Time waveforms

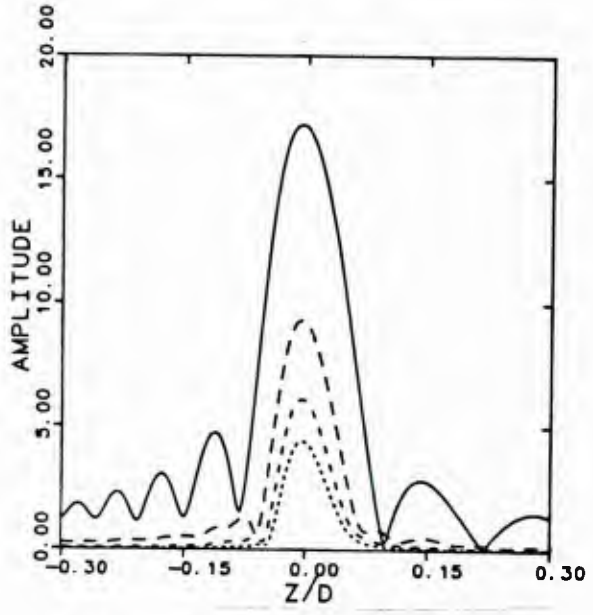

Figure 8

Axial amplitudes

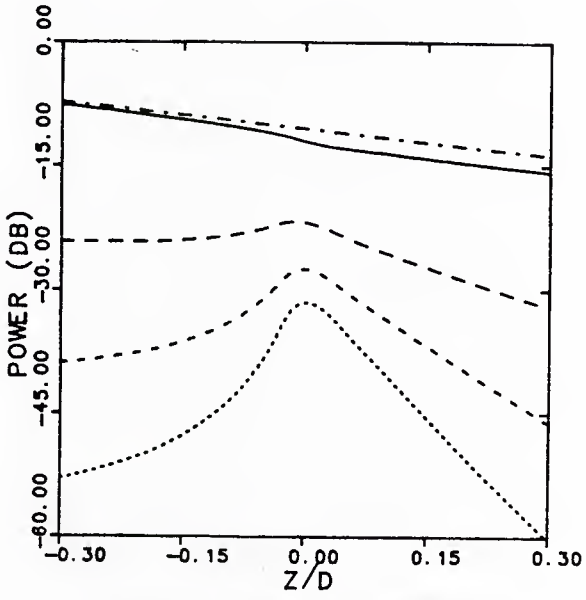

Figure 9

Power distributions

in the wave as a function of frequency. The total power in any given harmonic component is calculated by integrating the intensity of that component across the entire field. Shown in Fig. 9 is the distribution of power in the first four harmonic components of the waveform in Fig. 7. The reference value for the decibel scale is the total power transmitted by the source. For comparison, the dot-dash line in Fig. 9 is the result from linear theory, where all the energy remains in the fundamental component and decays as $e^{-2\alpha z}$. The (solid) curve for the fundamental component diverges from linear theory, particularly in the focal region, as energy is pumped into higher harmonics. However, the trend appears to reverse just beyond the focus. Energy is now depleted from the nonlinearly generated harmonics, although relatively little is apparently returned to the fundamental component. The change in direction of energy flow among the harmonic components is due initially to different phase shifts experienced by the various signals as they propagate through the focal region. Beyond the focus, spreading losses dramatically reduce the finite amplitude effects, and the energy in the harmonic components is lost to thermal and viscous mechanisms. It is interesting that the pronounced finite amplitude distortion observed on axis (Fig. 7) results from only a 2 dB overall loss of energy in the fundamental component. This "extra decibel" loss is the difference between the dot-dash and solid lines in Fig. 9.

Shown in Fig. 10 are beam patterns for the fundamental through fourth harmonic components in a focused sound field where $G = 50$, $\alpha d = 1.0$, and $d/l_p = 1.0$. The choice of $2Gu$ for the ordinate on the plots is motivated by the form of the linear solution for the amplitude distribution in the focal plane, $2J_1(2Gu)/2Gu$. Of particular significance is the intricate structure of the field near the focal plane. As in the farfield of unfocused circular sources, the second harmonic component has twice as many sidelobes as the fundamental component, the third harmonic has three times as many, and so on (see Ref. 29). The additional sidelobes have been referred to as *fingers* [32]. On the whole, the field structure near the focal plane is similar to that observed in the farfield. One noticeable difference concerns the positions of the nonlinearly generated sidelobes relative to the sidelobes of the fundamental component. In a focused sound field, the nonlinearly generated sidelobes appear slightly closer to the axis than do their counterparts in the farfield.

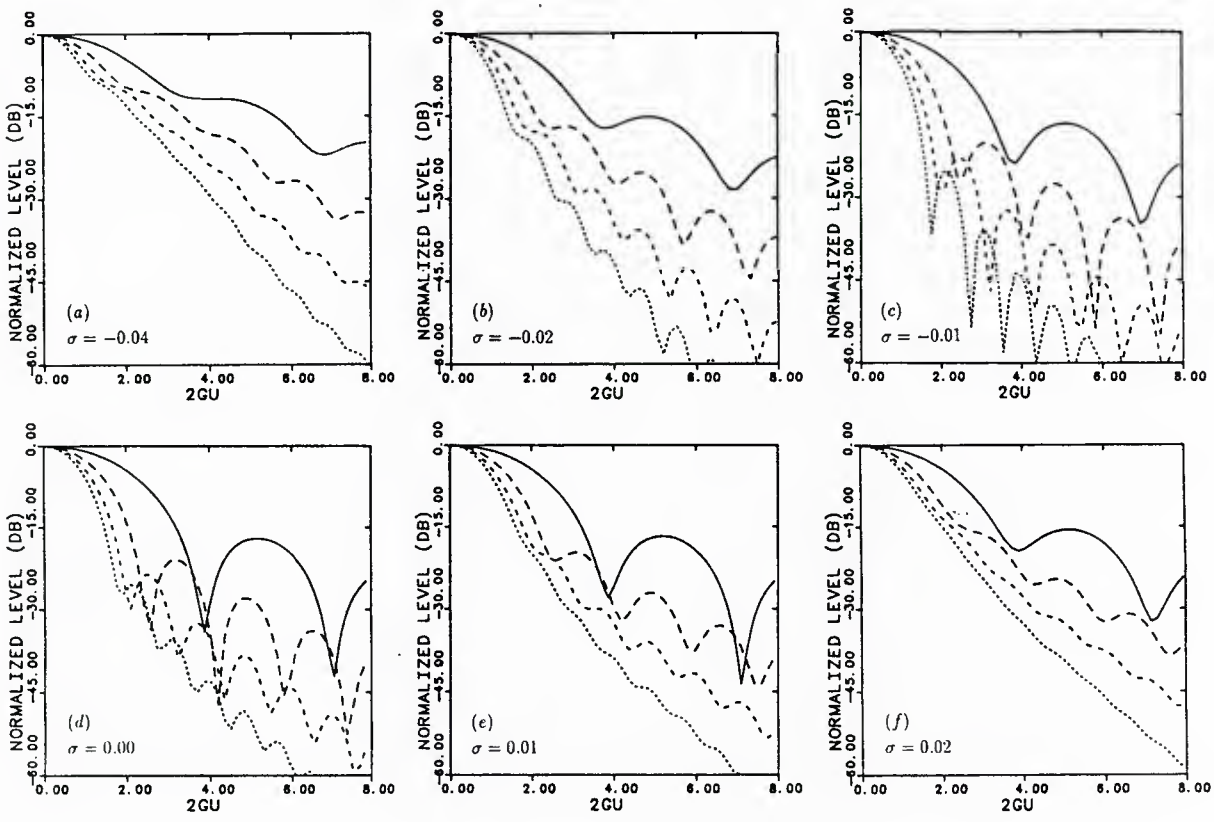

Figure 10

Beam patterns

III. NONCOLLINEAR TONE-NOISE INTERACTIONS

This project is an investigation of nonlinear effects that result from the noncollinear interaction of a pure tone sound wave with an acoustic noise field. The noncollinear interaction is produced in an experiment where acoustic noise in the plane wave mode of a rectangular duct interacts with a pure tone in the first higher order mode. Work on this project is being performed by Lind, who received support from ONR only during the period 1 January 1986 through 31 May 1986. All subsequent support has been provided by the National Science Foundation. However, the partial support provided by ONR was instrumental in getting the project started. The investigation is still in progress.

It should be noted that the problem of noncollinear interaction between a pure tone and noise is closely related to the measurement of noise with a parametric receiving array (see Sec. I).

A. Background

As discussed in the First Annual Summary Report [1], this project grew out of research on the nonlinear interaction of pure tones that propagate in different modes of a rectangular duct. The nonlinear interaction of waves that propagate in higher order modes of a rectangular duct may be deduced from an analysis of noncollinear plane wave interaction. In a two-dimensional duct, for example, any wave in a higher order mode may be decomposed into a pair of plane waves that propagate in different directions. This approach was followed by TenCate and Hamilton [33,34], who investigated both theoretically and experimentally the noncollinear interaction in a rectangular duct of two pure tones having different frequencies. Theory was shown to agree well with the measured sum and difference frequency components. The theory is extended in the present investigation to model the noncollinear interaction of a pure tone with noise.

Previous work by other researchers, both experimental and theoretical, has considered the collinear interaction of plane [35,36] and spherical [37] wave noise signals. The collinear interaction of noise with a finite amplitude tone has also been investigated [38]. In many cases of practical interest, however, acoustic noise cannot be modeled as an ideal plane or spherical wave. For example, the noise in jet engine ducts may propagate in a variety of modes, and ambient noise in reverberant environments may be essentially isotropic. No investigations known to the author consider the nonlinear interaction of noise in higher order modes of

waveguides. However, Refs. 39–41 analyze the nonlinear absorption of a pure tone by an isotropic noise field. The theory for the so-called absorption of sound by sound was derived by Westervelt [39]. Westervelt's theory also describes the sum and difference frequency sidebands produced by the interaction of the tone with the noise field. The nonlinearly generated sidebands of noise were measured by Stanton and Beyer [42,43] and shown to agree with Westervelt's predictions. However, extreme care was necessary for creating a purely isotropic noise field in the experiments. Departure from perfect isotropy resulted in measured sidebands whose shapes changed as a function of location in the interaction region. Such variations, which result from noncollinear interaction, are not predicted by Westervelt's model. Typical noise fields are neither collinear nor isotropic, and therefore an understanding of noncollinear interaction in noise fields is required.

B. Results

Our analysis is based on a theoretical model [34] developed for the weak nonlinear interaction of two pure tones in different modes of a rectangular duct. Here we shall consider the interaction of a wave of angular frequency ω_0 in the (1,0) (*i.e.*, the first higher order) mode with a wave of frequency ω in the (0,0) (*i.e.*, plane wave) mode. Shown in Fig. 11 is the experimental apparatus and associated geometry. For the primary wave field we write

$$p = p_0 e^{-\alpha_0 z} \cos(\pi x/a) \sin(\omega_0 t - k_0 z \cos\theta) + p_n e^{-\alpha_\omega z} \sin(\omega t - k_\omega z)\,, \tag{9}$$

where p_0 is the initial pressure amplitude of the tone at frequency $\omega_0/2\pi$, $k_0 = \omega_0/c_0$ the wavenumber, α_0 the attenuation coefficient, and a the width of the duct in the x direction. Likewise, p_n is the initial amplitude of the plane wave, $k_\omega = \omega/c_0$ its wavenumber, and α_ω its attenuation coefficient. The angle $\theta = \sin^{-1}(\pi/k_0 a)$ is formed by the direction of propagation of wave fronts in the (1,0) mode with the z axis.

The quasilinear solution for the complex pressure at the sum and difference frequency ($\omega_\pm = \omega_0 \pm \omega$) may be written

$$p_\pm = p_n h_\pm(\omega)\,, \tag{10}$$

where $h_\pm(\omega)$ is a dimensionless transfer function defined by [34]

$$h_\pm(\omega) = \pm \frac{p_0 \omega_\pm^2 \beta_\pm(\theta) \exp(-\alpha_\pm z - j\Delta_\pm z/2) \cos(\pi x/a)}{\rho_0 c_0^4 (k_\pm \cos\theta_\pm - j\alpha_\pm + \Delta_\pm/2)} \frac{\sin \Delta_\pm z/2}{\Delta_\pm} \exp(j\omega_\pm t - j k_\pm z \cos\theta_\pm)\,. \tag{11}$$

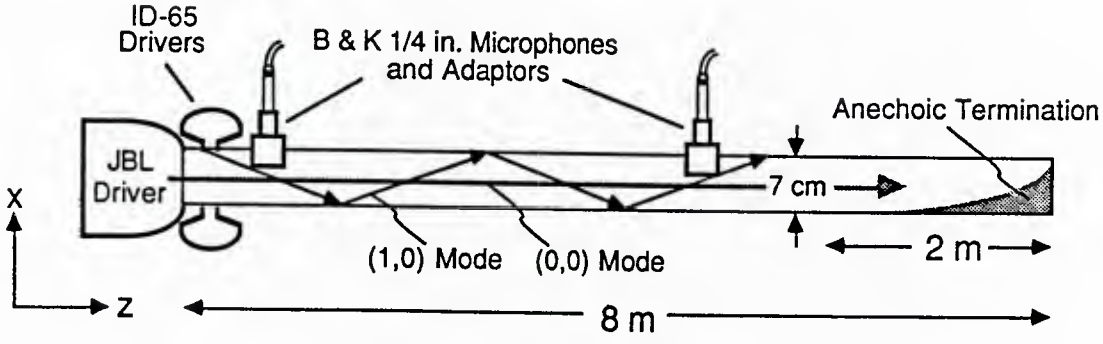

Figure 11

Waveguide apparatus

We have also defined a dispersion parameter $\Delta_\pm = (k_0 \cos\theta \pm k_\omega - k_\pm \cos\theta_\pm) - j(\alpha_0 + \alpha_\omega - \alpha_\pm)$, where $\theta_\pm = \sin^{-1}(\pi/k_\pm a)$ is the angle associated with the sum/difference frequency wave. The parameter $\beta_\pm(\theta)$ is a coefficient of nonlinearity that depends on the angle of interaction [44].

Extension to the case where a continuous spectrum of noise propagates in the plane wave mode is now straightforward. Let $\tilde{p}_n(\omega)$ denote the spectral distribution (having dimensions Pa/Hz) of the noise. Interaction of the noise with a pure tone in the (1,0) mode produces sum and difference frequency sidebands of noise having spectral distributions $\tilde{p}_\pm(\omega)$ defined by

$$\tilde{p}_\pm(\omega) = \tilde{p}_n(\omega) h_\pm(\omega) . \tag{12}$$

The quasilinear solution for the nonlinear interaction is thus interpreted on the basis of linear system theory.

Experimental verification of Eq. (12) is shown in Figs. 12 and 13. The source configuration shown in Fig. 11 was used to generate a pure tone at 3000 Hz in the (1,0) mode ($\theta = 55°$) and a band of noise centered at 350 Hz in the plane wave mode. The computer plots in Figs. 12 and 13 are theoretical predictions, and the photographs are experimental results. The nonlinearly generated sidebands of sum and difference frequency noise are seen to the right and left, respectively, of the spectral line at 3000 Hz. All spectra, theoretical and experimental, correspond to measurements along the upper wall of the duct ($x = a$).

Theory and experiment are seen to be in good agreement with regard to both the shapes and amplitudes of the sidebands. Note that the farther we are from the source ($z = 2.7$ m in Fig. 12 and $z = 5.4$ m in Fig. 13), the more scalloped in appearance are the sidelobe spectra. The scallops are due to the noncollinearity of the interacting waves. The results may be compared with Westervelt's prediction [39] for a pure tone in an isotropic noise field. The Westervelt model predicts sidelobes whose amplitudes increase with range and whose shapes remain the same. In contrast, Eq. (12) predicts sidelobes whose overall amplitudes decrease slightly because of absorption, and whose shapes become more scalloped as the range is increased. Thus the effects of noncollinear interaction are markedly different from interaction with an isotropic noise field.

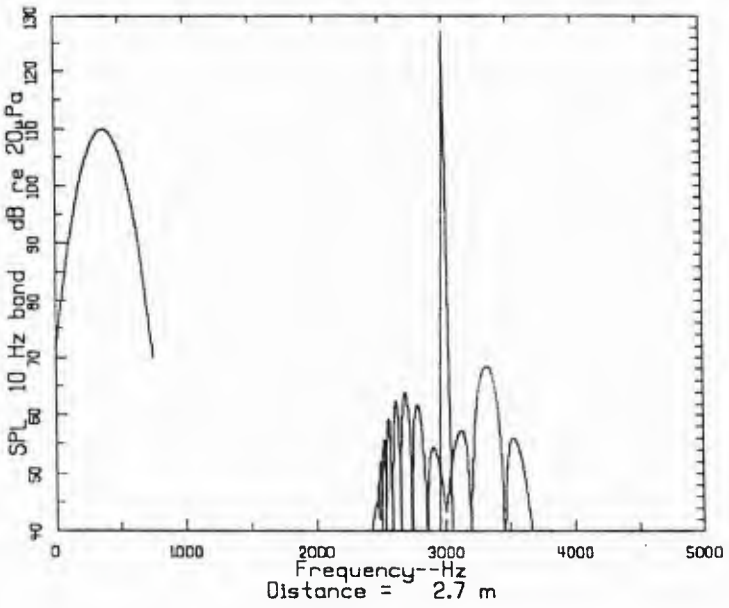

theory

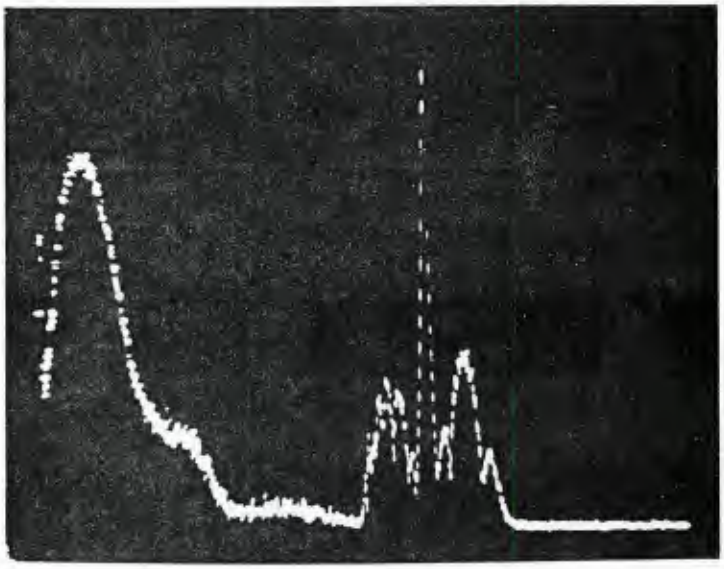

experiment

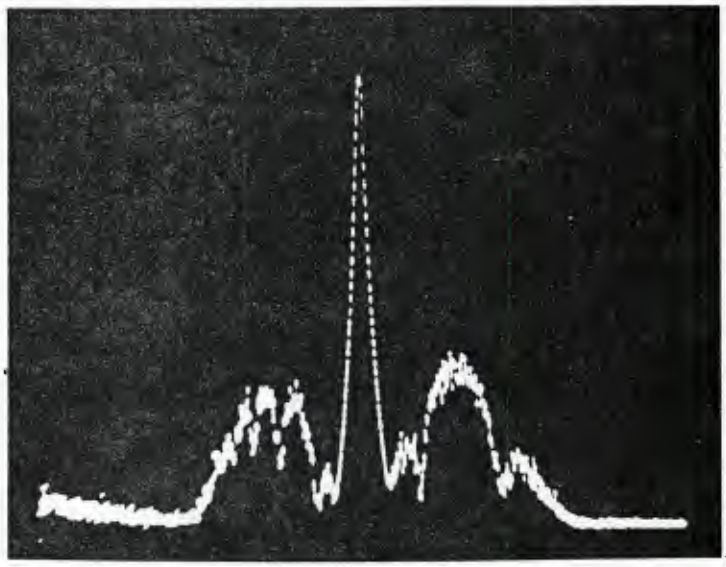

expanded scale
about 3000 Hz

Figure 12

Spectra at z = 2.7 m

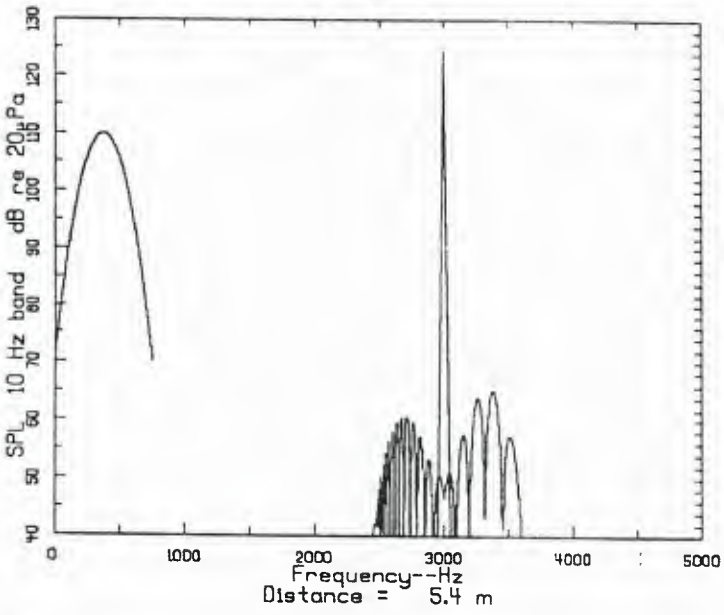

theory

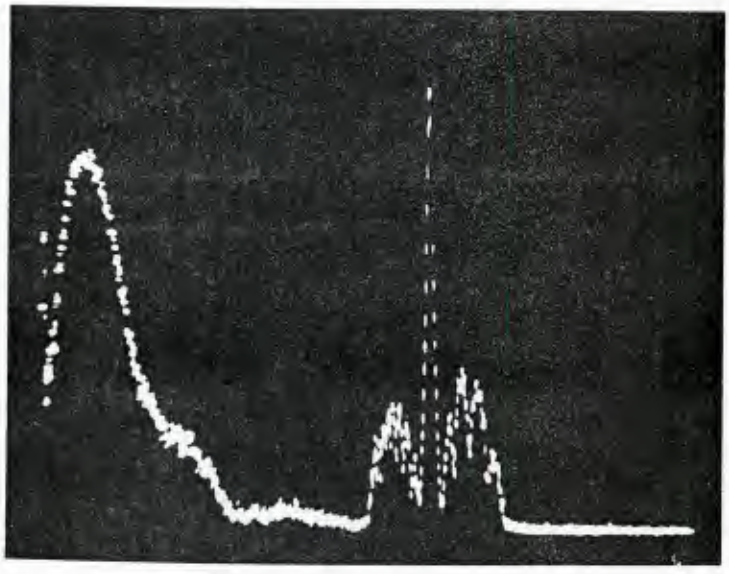

experiment

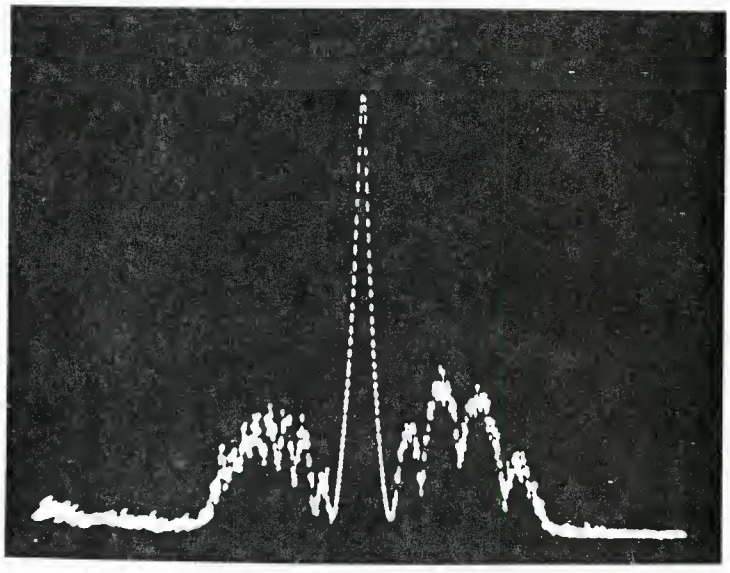

expanded scale
about 3000 Hz

Figure 13

Spectra at z = 5.4 m

REFERENCES

[1] M. F. Hamilton, "Problems in Nonlinear Acoustics: Parametric Receiving Arrays, Focused Finite Amplitude Sound, and Dispersive Nonlinear Interactions," First Annual Summary Report under ONR Contract N00014-85-K-0708, Department of Mechanical Engineering, The University of Texas at Austin, April 1986.

[2] N. P. Chotiros, "Noise Measurement in the Presence of Multipath Propagation," Progress Report No. 6, Contract AT/2027/0114 ARL, Department of Electronic and Electrical Engineering, University of Birmingham (1981).

[3] P. H. Rogers, A. L. Van Buren, A. O. Williams, Jr., and J. M. Barber, "Parametric Detection of Low-Frequency Acoustic Waves in the Nearfield of an Arbitrary Directional Pump Transducer," *J. Acoust. Soc. Am.* **55**, 528–534 (1974).

[4] M. F. Hamilton, J. Naze Tjøtta, and S. Tjøtta, "Noncollinear Interaction of Two Sound Beams from Displaced Gaussian Sources, with Application to Parametric Receiving Arrays," *J. Acoust. Soc. Am.* (in press).

[5] K. G. Foote, J. Naze Tjøtta, and S. Tjøtta, "Performance of the Parametric Receiving Array: Effects of Misalignment," *J. Acoust. Soc. Am.* (in press).

[6] J. D. Sample, "Gaussian Models for Complex Sound Sources in the Paraxial Region," *J. Acoust. Soc. Am.* (in press).

[7] J. D. Sample, "A Technique for Calculating the Nonlinear Interaction of Arbitrary Directional Sound Sources in the Paraxial Region," *J. Acoust. Soc. Am.* (in press).

[8] C. M. L. Darvennes and M. F. Hamilton, "Parametric Wave Interactions near Reflecting Surfaces," *J. Acoust. Soc. Am.* **80**, S105 (1986).

[9] B. K. Novikov, V. I. Tarasov, and V. I. Timoshenko, "Behavior of the Characteristics of a Parametric Radiator near a Reflecting Boundary," *Sov. Phys.–Acoust.* **29**, 138–142 (1983).

[10] D. M. Donskoi, L. A. Ostrovskii, and A. M. Sutin, "Aspects of Parametric Amplification and Reception of Acoustic Waves," *Sov. Phys.–Acoust.* **27**, 256–257 (1981).

[11] D. M. Donskoi and A. M. Sutin, "Parametric Reception of Acoustic Signals in Inhomogeneous Media," *Sov. Phys.–Acoust.* **27**, 485–487 (1981).

[12] D. M. Donskoi, V. A. Zverev, and A. I. Kalachev, "Parametric Selection of Sound Rays in Inhomogeneous Media," *Sov. Phys.–Acoust.* **29**, 106–108 (1983).

[13] R. T. Beyer, *Nonlinear Acoustics* (Naval Sea Systems Command, Washington, DC, 1974), pp. 299–311.

[14] R. T. Beyer, *Nonlinear Acoustics in Fluids* (Van Nostrand Reinhold, New York, 1984), pp. 228–298.

[15] U. Ingard and D. C. Pridmore-Brown, "Scattering of Sound by Sound," *J. Acoust. Soc. Am.* **28**, 367–369 (1956).

[16] P. J. Westervelt, "Scattering of Sound by Sound," *J. Acoust. Soc. Am.* **29**, 934–935 (1957).

[17] J. L. S. Bellin and R. T. Beyer, "Scattering of Sound by Sound," *J. Acoust. Soc. Am.* **32**, 339–341 (1960).

[18] J. P. Jones and R. T. Beyer, "Scattering of Sound by Sound," *J. Acoust. Soc. Am.* **48**, 398–402 (1970).

[19] P. J. Westervelt, "Recent Advances in the Theory of the Nonscattering of Sound by Sound," in *Proceedings of the 10th International Symposium on Nonlinear Acoustics*, edited by A. Nakimura (Teikohsha Press, Kadoma, Japan, 1984), pp. 117–120.

[20] R. N. McDonough, "Long-Aperture Parametric Receiving Arrays," *J. Acoust. Soc. Am.* **57**, 1150–1155 (1975).

[21] N. S. Bakhvalov, Ya. M. Zhileikin, E. A. Zabolotskaya, and R. V. Khokhlov, "Focused High-Amplitude Sound Beams," *Sov. Phys.–Acoust.* **24**, 10–15 (1978).

[22] N. S. Bakhvalov, Ya. M. Zhileikin, E. A. Zabolotskaya, *Nonlinear Theory of Sound Beams* (American Institute of Physics, New York, 1987).

[23] E. A. Zabolotskaya and R. V. Khokhlov, "Quasi-plane Waves in the Nonlinear Acoustics of Confined Beams," *Sov. Phys.–Acoust.* **15**, 35–40 (1969).

[24] V. P. Kuznetsov, "Equations of Nonlinear Acoustics," *Sov. Phys.–Acoust.* **16**, 467–470 (1971).

[25] B. G. Lucas and T. G. Muir, "The Field of a Focusing Source," *J. Acoust. Soc. Am.* **72**, 1289–1296 (1982).

[26] B. G. Lucas and T. G. Muir, "The Field of a Finite-Amplitude Focusing Source," *J. Acoust. Soc. Am.* **74**, 1522–1528 (1983).

[27] T. S. Hart and M. F. Hamilton, "Nonlinear Effects in Focused Sound Fields," *J. Acoust. Soc. Am.* **81**, S25 (1987).

[28] T. S. Hart and M. F. Hamilton, "Nonlinear Effects in Focused Sound Fields," *Proceedings of the 11th International Symposium on Nonlinear Acoustics*, 24–28 August 1987, Novosibirsk, USSR (in press).

[29] M. F. Hamilton, J. Naze Tjøtta, and S. Tjøtta, "Nonlinear Effects in the Farfield of a Directive Sound Source," *J. Acoust. Soc. Am.* **78**, 202–216 (1985).

[30] S. I. Aanonsen, "Numerical Computation of the Nearfield of a Baffled Piston Transducer," Rep. No. 73, Department of Mathematics, University of Bergen, Bergen, Norway (1983).

[31] D. Rugar, "Resolution Beyond the Diffraction Limit in the Acoustic Microscope: A Nonlinear Effect," *J. Appl. Phys.* **56**, 1338–1346 (1984).

[32] J. Berntsen, J. Naze Tjøtta, and S. Tjøtta, "Nearfield of a Large Acoustic Transducer. Part IV: Second Harmonic and Sum Frequency Radiation," *J. Acoust. Soc. Am.* **75**, 1383–1391 (1984).

[33] J. A. TenCate and M. F. Hamilton, "Dispersive Nonlinear Wave Interactions in a Rectangular Duct," in *Proceedings of the 12th International Congress on Acoustics*, Toronto, Canada, July 1986 (Beauregard Press, Ottawa), Vol. 1, paper C6-2.

[34] M. F. Hamilton and J. A. TenCate, "Sum and Difference Frequency Generation due to Noncollinear Wave Interaction in a Rectangular Duct," *J. Acoust. Soc. Am.* **81**, 1703–1712 (1987).

[35] F. M. Pestorious and D. T. Blackstock, "Propagation of Finite-Amplitude Noise," in *Finite-Amplitude Wave Effects in Fluids*, Proceedings of the 1973 Symposium, Copenhagen, edited by L. Bjørnø, (IPC Science and Technology, Guildford, England, 1974), pp. 24–29.

[36] L. Bjørnø and S. N. Gurbatov, "Evolution of Universal High-Frequency Asymptotic Forms of the Spectrum in the Propagation of High-Intensity Acoustic Noise," *Sov. Phys.–Acoust.* **31**, 179–182 (1985).

[37] D. A. Webster and D. T. Blackstock, "Experimental Investigation of Outdoor Propagation of Finite-Amplitude Noise," NASA Contractor Rep. 2992, Langley Research Center (1978).

[38] D. A. Webster and D. T. Blackstock, "Collinear Interaction of Noise with a Finite-Amplitude Tone," *J. Acoust. Soc. Am.* **63**, 687–693 (1978).

[39] P. J. Westervelt, "Absorption of Sound by Sound," *J. Acoust. Soc. Am.* **59**, 760–764 (1976) [First appeared in *J. Acoust. Soc. Am.* **53**, 384(A) (1973)].

[40] V. A. Krasili'nikov, O. V. Rudenko, and A. S. Chirkin, "Absorption of Low-Amplitude Sound due to Interaction with Noise," *Sov. Phys.–Acoust.* **21**, 80–81 (1975).

[41] V. I. Pavlov, "Sound Absorption in a Noisy Medium," *Sov. Phys.–Acoust.* **22**, 322–325 (1977).

[42] T. K. Stanton and R. T. Beyer, "The Interaction of Sound with Noise in Water," *J. Acoust. Soc. Am.* **64**, 1667–1670 (1978).

[43] T. K. Stanton and R. T. Beyer, "The Interaction of Sound with Noise in Water II," *J. Acoust. Soc. Am.* **69**, 989–992 (1981).

[44] M. F. Hamilton and D. T. Blackstock, "On the Coefficient of Nonlinearity β in Nonlinear Acoustics," *J. Acoust. Soc. Am.* (in press).